

# Electropolymerization of iron tetra(*o*-aminophenyl) porphyrin from aqueous solution and the electrocatalytic behavior of modified electrode

Shen-Ming Chen · Ying-Lu Chen · R. Thangamuthu

Received: 2 August 2006 / Revised: 16 March 2007 / Accepted: 22 March 2007 / Published online: 21 April 2007  
© Springer-Verlag 2007

**Abstract** Stable electroactive iron tetra(*o*-aminophenyl) porphyrin (FeTAPP) films are prepared by electropolymerization from aqueous solution by cycling the electrode potential between  $-0.4$  and  $1.0$  V vs Ag/AgCl at  $0.1$  V s $^{-1}$ . The cyclic voltammetric response indicates that polymerization takes place after the oxidation of amino groups, and the films could be produced on glassy carbon (GC) and gold electrodes. The film growth of poly(FeTAPP) was monitored by using cyclic voltammetry and electrochemical quartz crystal microbalance. The cyclic voltammetric features of Fe(III)/Fe(II) redox couple in the film resembles that of surface confined redox species. The electrochemical response of the modified electrode was found to be dependent on the pH of the contacting solution with a negative shift of  $57$  mV/pH. The electrocatalytic behavior of poly(FeTAPP) film-modified electrode was investigated towards reduction of hydrogen peroxide, molecular oxygen, and chloroacetic acids (mono-, di-, and tri-). The reduction of hydrogen peroxide, molecular oxygen, and dichloroacetic acid occurred at less negative potential on poly(FeTAPP) film compared to bare GC electrode. Particularly, the overpotential of hydrogen peroxide was reduced substantially. The O $_2$  reduction proceeds through direct four-electron reduction mechanism.

**Keywords** FeTAPP · Electropolymerization · Modified electrode · Electrocatalysis · Oxygen · Chloroacetic acids

## Introduction

Over the past two decades, electrodes coated with electroactive polymers have been the focus of intensive research interest due to their many potential applications in widely differing areas like energy conversion and storage, electrocatalysis, electroanalysis, electrochromism, molecular electronics, biosensor, and as a media for controlled drug release [1–5]. Polymer coatings are usually prepared either by applying preformed polymer or polymerizing the monomer directly on the electrode surface. Among these, the latter approach is attractive, as we can easily control the thickness, permeation, and charge transport characteristics of the resulting polymer film by simply adjusting the experimental conditions of electrochemical polymerization [6]. In this direction, modifying the surface of conventional electrodes with transition metal macrocyclic complexes is attractive in several grounds. In particular, special attention has been focused on metalloporphyrin- and metallophthalocyanine-based films [7–10].

One way to electropolymerize a desired electroactive macrocyclic monomer is to functionalize its periphery with groups, which becomes activated to polymeric coupling reactions by electroreduction or oxidation of the monomer. For example, Macor and Spiro [11] have prepared metallo (protoporphyrin IX) polymeric film-coated electrode by oxidative electropolymerization. Similarly, aniline-substituted porphyrins and their derivatives can be electropolymerized [8, 12–15]. In particular, tetra(amino) phenylporphyrins were used in the earlier studies to realize surface-modified electrodes [12] due to the fact that oxidations of aromatic compounds bearing electron-donating substituents are known [16] to generally lead to coupling reactions and often polymeric products. A well-known example is oxidative electropolymerization of

S.-M. Chen (✉) · Y.-L. Chen · R. Thangamuthu  
Department of Chemical Engineering and Biotechnology,  
National Taipei University of Technology,  
No. 1, section 3, Chung-Hsiao East Road,  
Taipei, Taiwan 106, Republic of China  
e-mail: smchen78@ms15.hinet.net

aniline [17, 18], where formation of the radical cation follows head-to-tail coupling between the amine group and *para*- and *ortho*- ring positions. As expected, analogous coupling reactions took place during electropolymerization of tetra(amino)phenylporphyrins, which lead to polymeric film formation on the electrode surface [12]. Except for a few, electropolymerization of porphyrins was mostly carried out in a nonaqueous medium, but in the present study, it is performed in an aqueous medium using iron tetra(*o*-aminophenyl)porphyrin (FeTAPP).

Use of porphyrin- and metalloporphyrin-modified electrodes in electrocatalysis has been known for the last several years. In particular, attention has been focused on electrocatalytic reduction of oxygen and hydrogen peroxide due to their relevance to fuel cell application [19–22]. Usually, oxygen is reduced in a two-electron process to hydrogen peroxide, and this is often followed at more negative potentials by a further two-electron reduction of hydrogen peroxide to water. The four-electron reduction of water, which is more desirable from the viewpoint of fuel cell application, has been observed in a number of cases and involves iron and cobalt porphyrins [19–21]. However, a great deal of interest still exists in the development of new catalysts capable of effecting direct four-electron reduction of oxygen to water. Similarly, porphyrin-modified electrodes have been used advantageously in electroanalysis. For example, iron and cobalt porphyrin-coated electrodes were used for the detection of organohalides [23, 24].

In the present investigation, we have described the preparation of poly(FeTAPP) films by means of potentiodynamic method from an aqueous medium. The electrochemical properties and electrocatalytic behavior of poly(FeTAPP) film-modified electrodes towards reduction of hydrogen peroxide, oxygen, and chloroacetic acids (mono-, di-, and tri-) were studied.

## Experimental

Iron tetra(*o*-aminophenyl)porphyrin purchased from Porphyrin Products (Logan, Utah, USA) was used as received. All other chemicals used were of analytical grade and used without further purification. Aqueous solutions of pH 0.5 to 2 were prepared from 0.1 M Na<sub>2</sub>SO<sub>4</sub> by adjusting the pH with sulfuric acids, whereas pH 5 solution was prepared from 0.1 M Na<sub>2</sub>SO<sub>4</sub> and 0.01 M KHP then pH adjusted with NaOH. Solutions were prepared using doubly distilled deionized water and then deaerated by purging with high purity nitrogen gas for about 20 min before performing electrochemical experiments. In addition, a continuous flow of nitrogen over the aqueous solution was maintained during measurements.

The electrochemical experiments were carried out with Bioanalytical system (Model CV-50 W) and CH Instruments (Model CHI-400). Cyclic voltammograms were recorded in a three-electrode cell configuration in which a BAS glassy carbon electrode (GCE; area=0.07 cm<sup>2</sup>) was used as working electrodes. The auxiliary compartment contained a platinum wire that was separated by a medium-sized glass frit. All cell potentials were recorded using either Ag|AgCl|KCl (sat) or Hg/Hg<sub>2</sub>Cl<sub>2</sub>/KCl (sat) reference electrode. Rotating disc electrode (RDE) and amperometric experiments were performed using PINE Instrument (USA) in conjunction with CHI-750 potentiostat connected to a Model AFMSRX analytical rotator. The rotating ring-disk electrode (RRDE) consisted of a GC disk electrode and a platinum ring electrode.

The working electrode for the electrochemical quartz crystal microbalance (EQCM) measurements was an 8 MHz AT-cut quartz crystal with gold electrodes. The diameter of the quartz crystal was 13.7 mm, and it was 5 mm for the gold electrode.

The flow injection analysis system consisted of a carrier reservoir, a Cole Parmer Masterflex microprocessor pump drive, a Rehodyne 7125 sample injection valve (20- $\mu$ l loop), interconnecting Teflon tubing, and a BAS CC-5 type electrochemical injector (West Lafayette, IN).

Poly(FeTAPP) films were potentiodynamically grown on GC working electrode by cycling the potential at a scan rate of 50 mV s<sup>-1</sup> between 0.2 and 1.2 V vs Ag/AgCl in H<sub>2</sub>SO<sub>4</sub> buffer solution of pH 1 containing 0.1 mM FeTAPP monomer. Before modification, GCE was polished with 0.05  $\mu$ m alumina on Buehler felt pads and then ultrasonically cleaned for about a minute in water. Finally, the electrode was washed thoroughly with double distilled water and used. After film formation, the electrode was rinsed with distilled water and used for further characterization.

## Results and discussion

### Potentiodynamic electropolymerization of FeTAPP in an aqueous medium

The current–voltage behavior recorded during potentiodynamic electropolymerization of FeTAPP monomer at GCE is presented in Fig. 1. The irreversible oxidation of the amino groups (an anodic wave starting at about 0.85 V) gives origin to the electropolymerization of this macrocyclic compound. This means that the oxidation of amino groups is a key step in the electropolymerization mechanism [25–27]. The mechanisms of electropolymerization of conjugated macrocycles with amino substituents has been described normally as the formation of a radical cation centered in the amino group that diffuses to the solution where it attacks a

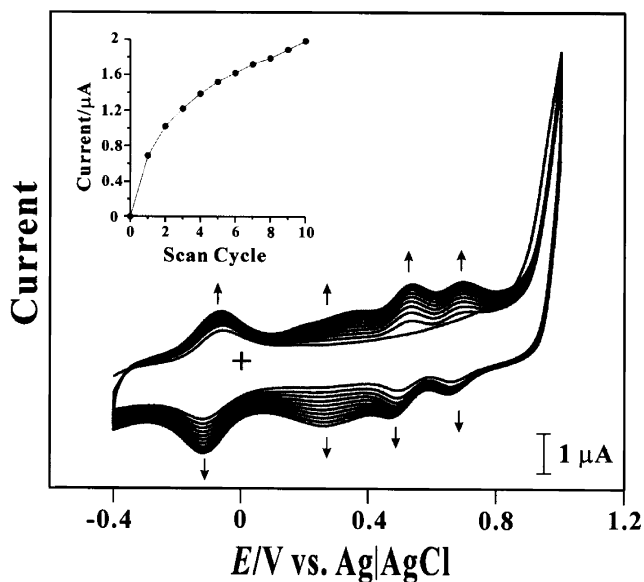


**Fig. 1** Cyclic voltammetric response of the electropolymerization of FeTAPP, (about 0.1 mM) on GCE from  $\text{H}_2\text{SO}_4$  buffer solution of pH 1. Scan rate:  $0.1 \text{ V s}^{-1}$ . The inset shows variation of the anodic peak current ( $I_{\text{pa}}$ ) of the peak appearing at  $E_{\text{pa}}=0.52 \text{ V}$  with number of potential scans

neutral molecule in a carbon of the phenyl substituent (in this case) or a radical cation forming a neutral dimer [26]. Therefore, chemical composition and electropolymerization mechanism of poly(FeTAPP) film formation is considered similar to that of polyaniline and its analogues [17, 18]. In the first scan, besides the amino group oxidation, the monomer exhibited a redox couple at  $-0.15 \text{ V}$  corresponding to the iron oxidation. The cyclic voltammograms in the subsequent scans showed four obvious redox couples approximately at  $+0.70$ ,  $+0.50$ ,  $+0.30$ , and  $-0.15 \text{ V}$ . The formal potential ( $E^{\circ'}$ ) found at  $0.68 \text{ V}$  corresponds to electrochemical redox couple of porphyrin ring, whereas  $E^{\circ'}$  of  $0.49$  and  $0.3 \text{ V}$  arose from the polymer bridge functional group [13, 28]. The more negative formal potential of  $-0.15 \text{ V}$  corresponds to Fe(II)/Fe(III) redox transition [14, 29]. The inset of Fig. 1 depicts how the anodic peak current ( $I_{\text{pa}}$ ) of the peak appearing at  $E_{\text{pa}}=0.52 \text{ V}$  changes with number of potential scans. The increase in peak current with scan number indicates the growth of electroactive poly(FeTAPP) film on GCE.

The electrosynthesis of poly(FeTAPP) has been monitored by EQCM. Figure 2 illustrates the simultaneously recorded voltammetry and EQCM data for poly(FeTAPP) film. The increase in the voltammetric peak current in Fig. 2a and the frequency decrease (or mass increase) in Fig. 2b are in agreement with the growth of poly(FeTAPP) film on the gold electrode. Using the Sauerbrey equation [30], change in mass of working electrode during the

electropolymerization was determined from the changes in the resonant frequency of microbalance. In the present investigation, the mass increase during the first and sixth scans was about  $430$  and  $1,650 \text{ ng/cm}^2$ , respectively, suggesting steady growth of poly(FeTAPP) film with number of scans.

It is clear from the above results that number of peaks, shapes, and locations are different depending on the nature of electrode material. These differences suggest the occurrence of strong interactions between the resulting polyporphyrins and the electrode surface. An analogous behavior was observed in other similar systems [31].

#### Electrochemical characterization of poly(FeTAPP) films

Figure 3 shows a series of cyclic voltammograms recorded in the potential range of  $0.03$  to  $-0.25 \text{ V}$  with poly(FeTAPP) film-modified GCE in  $\text{H}_2\text{SO}_4$  buffer solution (pH 1.5) at different scan rates. The modified electrode exhibited a reversible redox couple in this potential range with a formal potential of about  $-0.12 \text{ V}$ . As shown in the inset, the anodic peak current ( $I_{\text{pa}}$ ) varies linearly with scan rate. Thus, the electron transfer process can be interpreted

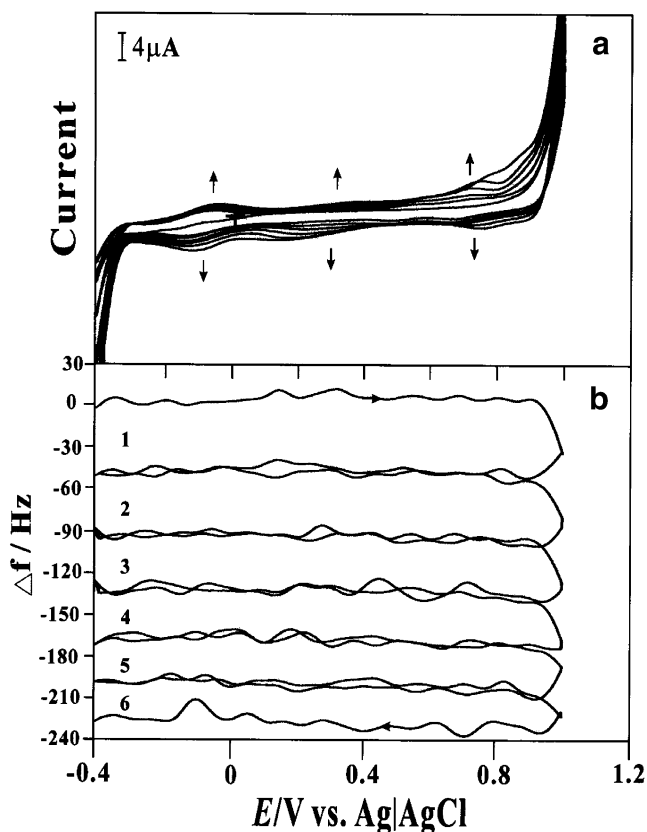


**Fig. 2** a Repetitive cyclic voltammograms of a gold electrode in  $\text{H}_2\text{SO}_4$  buffer solution of pH 1 containing  $1 \times 10^{-4} \text{ M}$  FeTAPP. Scan rate:  $0.02 \text{ V s}^{-1}$ . b Change in the frequency of EQCM recorded concurrently during first six consecutive cyclic voltammograms

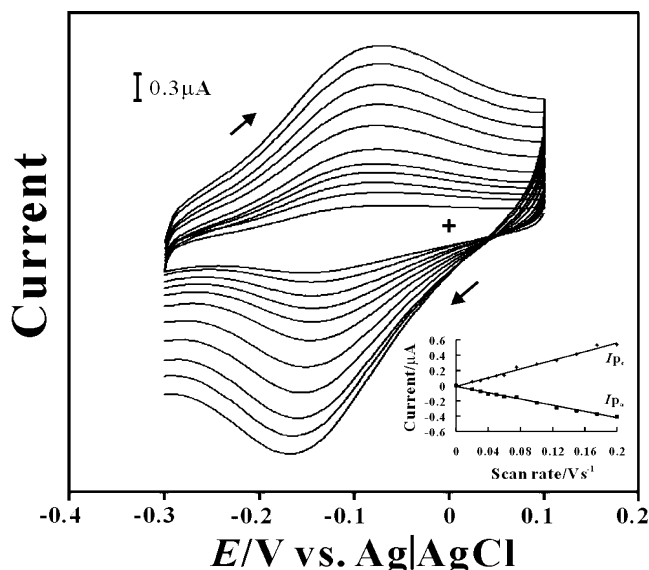


**Fig. 3** Cyclic voltammograms of poly(FeTAPP) film-modified GCE in  $\text{H}_2\text{SO}_4$  buffer solution of pH 1.5 at different scan rates. Inner to outer voltammograms correspond to scan rates of 20, 30, 40, 50, 60, 75, 100, 125, 150, 175, and 200  $\text{mV s}^{-1}$ , respectively. The inset shows variation of anodic peak current with scan rate

to be surface confined in the scan rate region studied [32, 33].

The redox switching behavior of poly(FeTAPP) film was assessed in  $\text{H}_2\text{SO}_4$  buffer solution (pH 1.5) using chronocoulometry technique. Figure 4 shows the redox switching of poly(FeTAPP) film-coated gold electrode between  $-0.4$  and  $0.4$  V with a pulse width of  $0.5$  s. Therefore, it takes  $1$  s to complete a double potential step, the process of stepping to the oxidized state and back to the reduced state

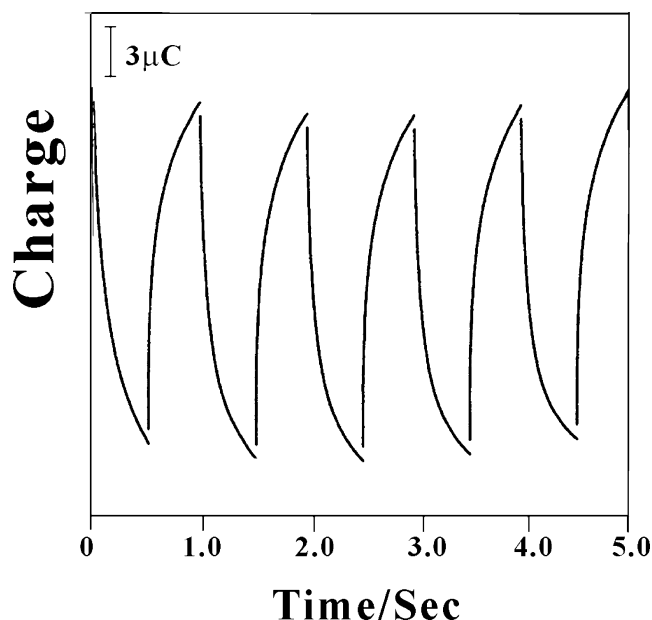


**Fig. 4** Chronocoulometry of poly(FeTAPP) film-coated gold electrode for the redox switching between  $-0.4$  and  $0.4$  V (vs Ag|AgCl) in  $\text{H}_2\text{SO}_4$  (pH 1.5) buffer solution with pulse width of  $0.5$  s

before switching to the oxidized state again. It is significant to note that the poly(FeTAPP) films have good reversibility and response time.

The electrochemical response of a poly(FeTAPP) film-coated electrode in buffer solutions of different pH values,  $0.5$  ( $\text{H}_2\text{SO}_4$ ),  $1$  ( $\text{H}_2\text{SO}_4$ ), and  $5$  ( $0.1$  M potassium hydrogen phthalate), are shown in Fig. 5. As observed for other electroactive polymeric coatings [34, 35], the electrochemical behavior of poly(FeTAPP) film is pH dependent. However, in general, all changes in cyclic voltammetric peak potentials and peak currents were reversible between pH  $0.5$  and  $5$ . The results indicate that the formal potential  $E^{0'}$ , which was estimated as the midpoint of reduction and oxidation peak potentials of Fe(III/II)TAPP redox couple, shows a linear relationship with pH in this pH range with a slope of  $-57$  mV/pH. This value is close to the theoretical value of  $-57$  mV/pH at  $20$  °C for the reversible one-electron transfer coupled by single-proton transportation [36, 37] suggesting that a single-proton transfer accompanies in the course of electron transfer reaction of Fe(III/II)TAPP redox couple. Thus, the simplified reaction for the Fe(III/II)TAPP redox reaction is given as follows:



where the charges on TAPP species are omitted.

Electrocatalytic behavior of poly(FeTAPP) film-modified electrode

Electrocatalytic behavior of poly(FeTAPP) film-modified electrode was investigated towards reduction of hydrogen peroxide, oxygen, and chloroacetic acids (mono-, di-, and tri-) using cyclic voltammetry and RRDE techniques.

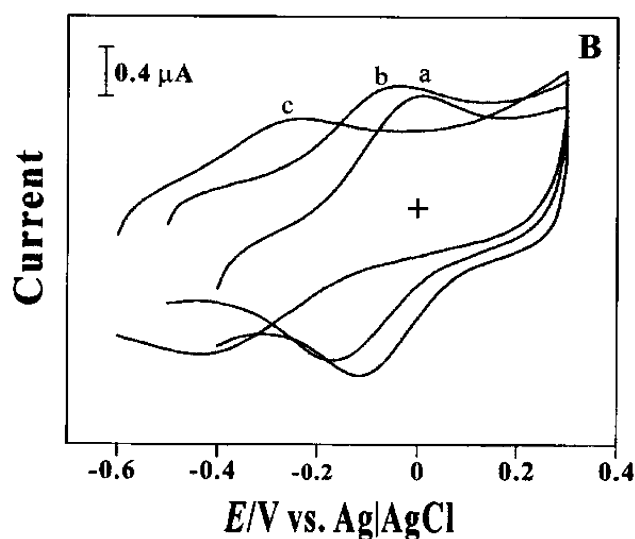


**Fig. 5** Cyclic voltammograms of poly(FeTAPP)-modified GCE in buffered solutions of different pH: *a*  $0.5$  ( $\text{H}_2\text{SO}_4$ ), *b*  $1$  ( $\text{H}_2\text{SO}_4$ ), and *c*  $5$  ( $0.1$  M potassium hydrogen phthalate). Scan rate:  $0.1$   $\text{V s}^{-1}$

### Mediated reduction of hydrogen peroxide

Because hydrogen peroxide is an intermediate product of oxygen reduction, investigating its reduction can help in understanding the reaction mechanisms. Figure 6 shows cyclic voltammograms of poly(FeTAPP) film-modified electrode in the presence (curves b–d) and absence (curve a) of  $\text{H}_2\text{O}_2$ . Curve a' represents the electrochemical reduction of  $\text{H}_2\text{O}_2$  on bare GCE. The cathodic peak potential for reduction of  $\text{H}_2\text{O}_2$  at modified electrode is about  $-0.04$  V, while at the bare electrode,  $\text{H}_2\text{O}_2$  is not reduced until  $-0.5$  V. Upon increasing the concentration of  $\text{H}_2\text{O}_2$ , cathodic peak current of Fe(III/II)TAPP redox transition increased enormously, and the anodic peak current decreases then disappears at higher substrate concentration. The cathodic peak current was found to increase linearly with the increase in  $\text{H}_2\text{O}_2$  concentration up to  $10$  mM. The decrease in overpotential and enhancement of peak current for  $\text{H}_2\text{O}_2$  reduction indicates strong catalytic effect of poly(FeTAPP) film towards  $\text{H}_2\text{O}_2$  reduction.

### Mediated reduction of molecular oxygen

Cyclic voltammetry studies were performed to investigate the effect of FeTAPP on the catalytic reduction of oxygen overpotential, and RDE and RRDE experiments were carried out to elucidate the mechanism of oxygen reduction. Figure 7 shows the cyclic voltammetric response of a bare GCE and poly(FeTAPP) film-coated GCE in  $\text{H}_2\text{SO}_4$  (pH 1)

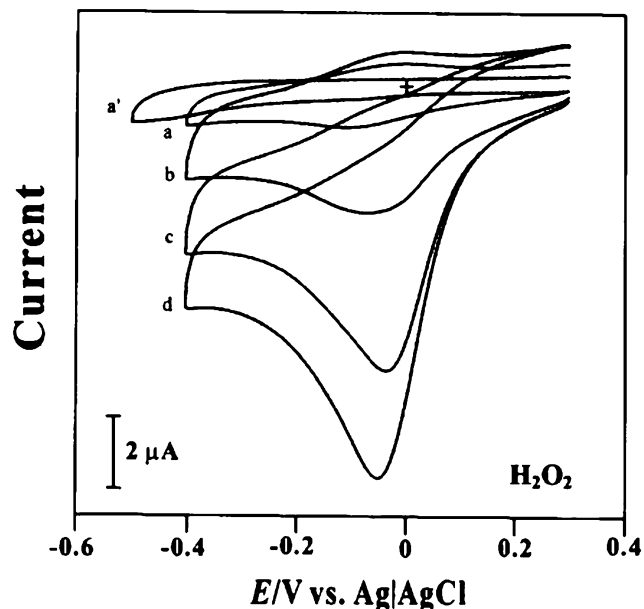


**Fig. 6** Cyclic voltammograms of poly(FeTAPP) film-coated electrode in  $\text{H}_2\text{SO}_4$  (pH 1) buffer solution containing different concentrations of  $\text{H}_2\text{O}_2$ : a 0; b  $2.5 \times 10^{-3}$ ; c  $7.5 \times 10^{-3}$ , and d  $10 \times 10^{-3}$  M. a' represents  $10 \times 10^{-3}$  M  $\text{H}_2\text{O}_2$  reduction on bare GCE. Scan rate:  $0.1 \text{ V s}^{-1}$

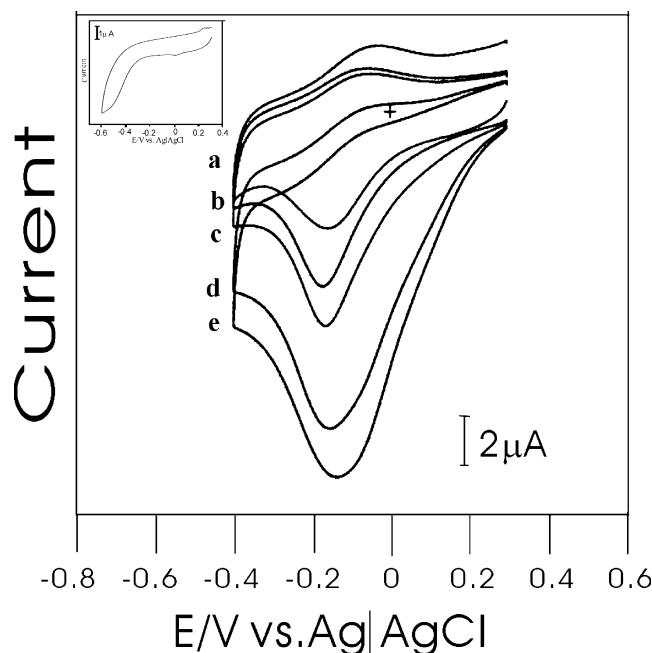


**Fig. 7** Cyclic voltammograms of poly(FeTAPP) film-coated electrode in  $\text{H}_2\text{SO}_4$  (pH 1) buffer solution containing different concentrations of  $\text{O}_2$ : a  $\text{N}_2$  saturated solution; b  $5 \times 10^{-5}$ ; c  $1 \times 10^{-4}$ ; d  $2 \times 10^{-4}$ , and e  $2.4 \times 10^{-4}$  M. Inset represents  $2.4 \times 10^{-4}$  M  $\text{O}_2$  reduction on bare GCE. Scan rate:  $0.1 \text{ V s}^{-1}$

buffer solution containing different concentrations of  $\text{O}_2$ . In nitrogen-saturated solution, the modified electrode exhibited a pair of reversible peaks corresponding to Fe (III/II) redox couple. As seen, the  $\text{O}_2$  reduction on bare electrode (inset) appears around  $-0.4$  V, while the reduction of  $\text{O}_2$  on the modified electrode occurs at the oxidation peak potential of the redox couple. In addition, the cathodic peak current is increased accordingly with increasing  $\text{O}_2$  concentration, and the anodic peak current decreases and disappeared eventually. Thus, a substantial decrease in overpotential and an enhancement of the peak current could be achieved with the modified electrode. This phenomenon indicates that the immobilized Fe(III/II)TAPP redox couple effectively mediated the  $\text{O}_2$  reduction reaction. In the earlier investigations, similar catalytic behavior was observed with this catalyst when dissolved in solution as well as covalently bound to the electrode surface [38] and immobilized on the electrode [39].

Rotating GCE coated with poly(FeTAPP) film as disc and platinum ring electrode were used to carry out RRDE experiments. Figure 8 shows RRDE responses of  $\text{O}_2$  reduction at the modified electrode. The potential of GC disc electrode was scanned from  $+0.3$  to  $-0.5$  V, while the platinum ring potential was kept at  $+0.85$  V to study the product of electrocatalytic reduction of oxygen and/or oxidize the  $\text{H}_2\text{O}_2$  generated by  $\text{O}_2$  reduction on the disc electrode. The lower curves represent the response of disc, i.e., the  $\text{O}_2$  reduction current, while the upper one

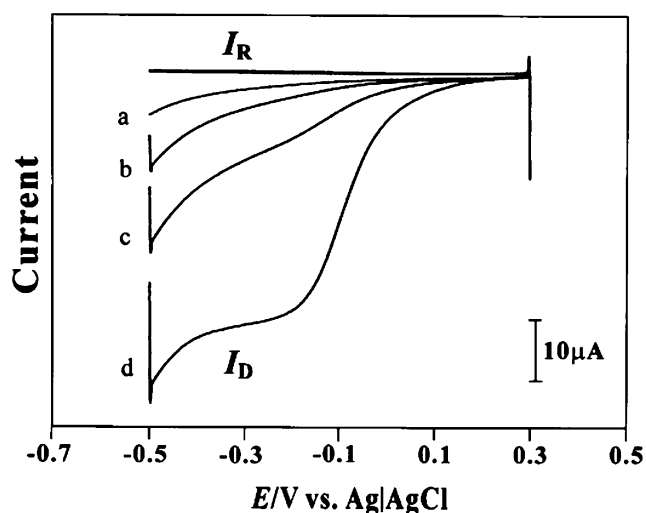


**Fig. 8** Current–potential curves for  $\text{O}_2$  reduction at a rotated GCE coated with poly(FeTAPP) film and platinum ring electrode in  $\text{H}_2\text{SO}_4$  (pH 1) buffer solution. Concentration of  $\text{O}_2$ : a 0, b  $2 \times 10^{-5}$ , c  $4 \times 10^{-5}$ , and d  $2.4 \times 10^{-4}$  M. Electrode was rotated at 2,500 rpm.  $E_R = +0.85$  V vs Ag/AgCl. Scan rate:  $0.015 \text{ V s}^{-1}$

corresponds to ring current. In all cases, a large disc current ( $I_D$ ) was observed for the modified electrode and the  $I_D$  value increases with  $\text{O}_2$  concentration. At the same time, the ring current ( $I_R$ ) was almost zero for all the  $\text{O}_2$  concentrations studied. Thus, the ratio of  $I_R/I_D$  was near zero for  $\text{O}_2$  reduction on poly(FeTAPP) film-modified electrode. The results suggest that  $\text{O}_2$  reduction proceeds on modified electrode along a pathway where  $\text{H}_2\text{O}$  was the major product, and very small amount of  $\text{H}_2\text{O}_2$  was formed. A similar reaction pathway, i.e., direct four-electron reduction of  $\text{O}_2$ , was reported by Bettelheim et al. [40] for polymer-bound FeTAPP-modified electrode at sufficiently

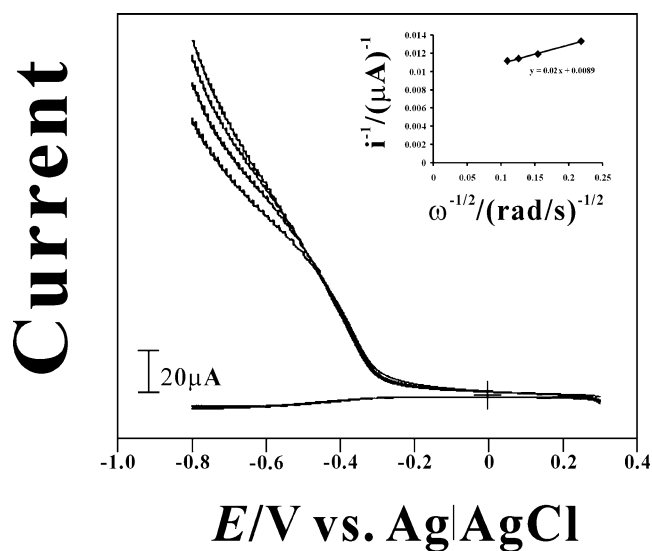


**Fig. 9** Current–potential curves for  $2.4 \times 10^{-4}$  M  $\text{O}_2$  reduction at poly(FeTAPP) film coated electrode in  $\text{H}_2\text{SO}_4$  (pH 1) buffer solution at different electrode rotation rate: 20, 40, 60, and 100 rpm. The inset shows a plot of  $I_D^{-1}$  vs  $(\text{rotation rate})^{-1/2}$

higher surface coverage. The current–potential response for  $2.4 \times 10^{-4}$  M oxygen reduction on FeTAPP-modified electrode at different electrode rotation rates demonstrates mixed current as shown in Fig. 9.

#### Mediated reduction of chloroacetic acids

It is well known that chloroacetic acids (mono-, di-, and tri-) can make grievous environmental contamination [41], consequently, determination of this kind of pollutants is very important in the environmental point of view. As mediated reduction of organohalides by electroreduced iron and cobalt porphyrins is known [23, 24, 42–45], we have evaluated the electrocatalytic behavior of poly(FeTAPP) film-modified electrodes towards chloroacetic acids (mono-, di-, and tri-). Figure 10a–c shows the cyclic voltammograms of poly(FeTAPP) film-modified electrodes in pH 1 buffer solution ( $\text{H}_2\text{SO}_4$ ) containing different concentrations of trichloroacetic acid (TCA), dichloroacetic acid (DCA) and

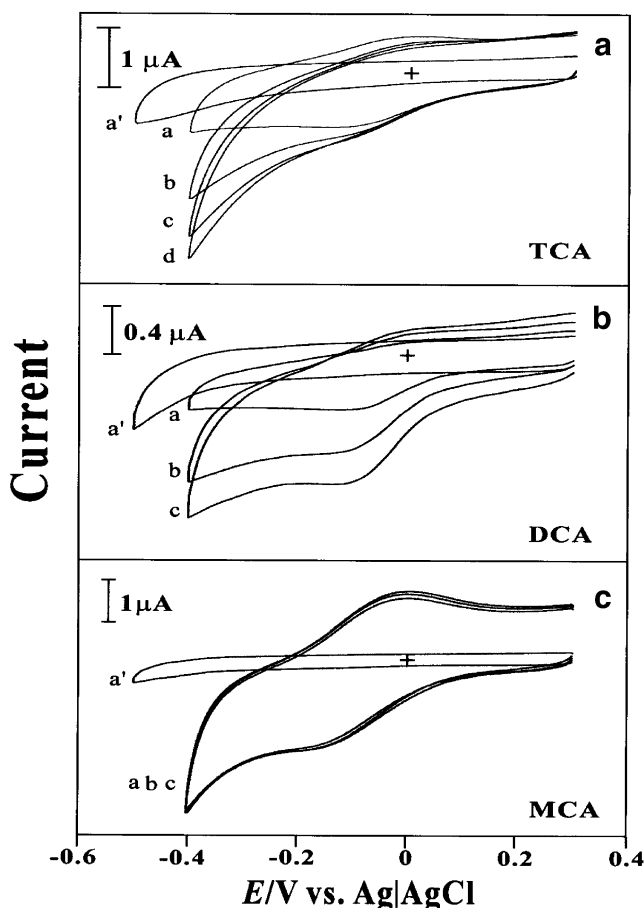
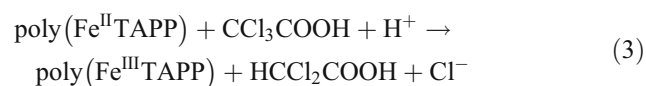


**Fig. 10** Cyclic voltammograms of poly(FeTAPP) film-coated electrode in  $\text{H}_2\text{SO}_4$  (pH 1) buffer solution containing different concentrations of  $\text{CCl}_3\text{COOH}$  (a): a 0, b  $5 \times 10^{-4}$ , c  $1.0 \times 10^{-3}$ , and d  $1.5 \times 10^{-3}$  M;  $\text{CHCl}_2\text{COOH}$  (b): a 0, b  $5 \times 10^{-4}$ , and c  $1 \times 10^{-3}$  M; and  $\text{CH}_2\text{ClCOOH}$  (c): a 0, b  $1.0 \times 10^{-3}$ , and c  $1.5 \times 10^{-3}$  M. a' in a, b, and c represents reduction of  $1.5 \times 10^{-3}$  M of all the three substrates on bare GCE. Scan rate:  $0.1 \text{ V s}^{-1}$

monochloroacetic acid (MCA), respectively. As shown in the figures, none of them reduced at bare GCE. However, the reduction current of modified electrode increases with increasing concentrations of both TCA and DCA, especially it is quite obvious with DCA. In addition, the anodic currents decreased simultaneously. In the case of DCA, reduction peak appeared at the reduction potential of Fe(III) of poly(FeTAPP) film, whereas the TCA reduced at higher negative potential. But there was no change in the current values of modified electrode when increasing the concentration of MCA. These observations collectively indicates that the poly(FeTAPP) film mediates the electrochemical reduction of TCA and DCA in the chloroacetic acid series studied. Especially, FeTAPP was an efficient catalyst for DCA reduction. Thus, the following reaction mechanism can be proposed for the electrocatalytic activity of poly(FeTAPP) film towards DCA and TCA reduction in acidic solution:



Although, at present, we have not realized a sensor, the above results promise for the design of new sensor in future for DCA and TCA based on poly(FeTAPP) film-modified electrodes. One of the advantages of constructing electrochemical sensor based on our modified electrode is that we never observed passivation phenomenon as opposite to myoglobin- and hemoglobin-embedded didodecyldimethylammonium bromide surfactant film-modified electrodes, which showed slight passivation during electrocatalytic reduction of organohalides including DCA [46]. Thus, the present study opens up a new possibility to develop low-cost sensor for organohalides.

## Conclusions

The oxidative electropolymerization of FeTAPP in aqueous solution gives rise to formation of stable electroactive film on electrode surfaces during repetitive potential cycling between  $-0.4$  and  $1.0$  V (Ag/AgCl). The oxidation of amino group is the key step in the electropolymerization. The pH dependence redox response of modified electrode

yields a slope of 57 mV per pH unit in the plot of formal potential vs pH suggesting a single-proton transfer accompanied during Fe(III/II)TAPP redox reaction. The poly(FeTAPP) film catalyzes the reduction of hydrogen peroxide, molecular oxygen, and DCA and TCA. The modified electrode diminishes the overpotential required for the reduction of hydrogen peroxide and DCA considerably compared to bare electrode. RRDE analysis shows that the  $\text{O}_2$  reduction proceeds on the modified electrode along a pathway where  $\text{H}_2\text{O}$  was the major product suggesting the occurrence of direct four-electron reduction. The present study opens up feasibility of utilizing poly(FeTAPP) film for developing low-cost sensor for organohalides.

**Acknowledgement** This work was financially supported by the National Science Council of the Taiwan (Republic of China).

## References

1. Snell KD, Keenan AG (1979) *Chem Soc Rev* 8:259
2. Murray RW (1980) *Acc Chem Res* 13:135
3. Murray RW (1983) In: Bard AJ (ed) *Electroanalytical chemistry*, vol 13. Marcel Dekker, NY, p 191
4. Murray RW (1992) *Molecular design of electrode surfaces. Techniques of chemistry series*, vol XXII. Wiley, New York
5. Leech D (1996) *Analytical applications of polymer-modified electrodes*. In: Lyons MEG (ed) *Electroactive polymers electrochemistry*, part 2, chap 10. Plenum, New York
6. Jin G, Zhang Y, Cheng W (2005) *Sens Actuators B* 107:528
7. Li H, Guarr TF (1991) *J Electroanal Chem* 317:189
8. Bedioui F, Devynck J, Bied-Charreton C (1995) *Acc Chem Res* 28:30
9. Ramirez G, Trollund E, Isaacs M, Armijo F, Zagal J, Costamagna J, Aguirre MJ (2002) *Electroanalysis* 14:540
10. Pontie M, Lecture H, Bedioui F (1999) *Sens Actuators B* 56:1
11. Macor KA, Spiro TG (1983) *J Am Chem Soc* 105:5601
12. White BA, Murray RW (1985) *J Electroanal Chem* 189:345
13. Bettelheim A, White BA, Raybuck SA, Murray RW (1987) *Inorg Chem* 26:1009
14. Bruti EM, Giannetto M, Mori M, Seeber R (1999) *Electroanalysis* 11:565
15. Armijo F, Isaacs M, Ramirez G, Trollund E, Canales J, Aguirre MJ (2004) *J Electroanal Chem* 566:315
16. Anderson JT, Stocker JH (1983) In: Baizer MM, Lund H (eds) *Organic electrochemistry*, 2nd edn. Marcel Dekker, New York, pp 691–726
17. Kobayashi T, Yoneyama H, Tamura H (1984) *J Electroanal Chem* 161:419
18. Kobayashi T, Yoneyama H, Tamura H (1984) *J Electroanal Chem* 177:293
19. Forshey PA, Kuwana T (1983) *Inorg Chem* 22:699
20. Shi C, Anson FC (1990) *Inorg Chem* 29:4298
21. Song E, Shi C, Anson FC (1998) *Langmuir* 14:4315
22. Khorasani-Motlagh M, Noroozifar M, Ghaemi A, Safari N (2004) *J Electroanal Chem* 565:115
23. Root DP, Pitz G, Priyantha N (1991) *Electrochim Acta* 36:855
24. Priyantha N, Weerabahu D (1996) *Anal Chim Acta* 320:263
25. Lucero M, Ramirez G, Riquelme A, Azocar I, Isaacs M, Armijo F, Forster JE, Trollund E, Aguirre MJ, Lexa D (2004) *J Mol Catal A Chem* 221:71
26. Chen S-M, Chen Y-LJ (2004) *J Electroanal Chem* 573:277

27. Armijo F, Carmen Goya M, Gimeno Y, Carmen Arevalo M, Jesus Aguirre M, Hernandez Creus A (2006) *Electrochem Commun* 8:779
28. Chidsey CED, Murray RW (1986) *Science* 231:25
29. Stone A, Fleischer EB (1968) *J Am Chem Soc* 90:2735
30. Brukenstein S, Shay M (1985) *Electrochim Acta* 30:1295
31. Armijo F, Goya MC, Reina M, Josefina Canales M, Arevalo MC, Aguirre MJ (2007) *J Mol Catal A Chem* 268:148
32. Bard AJ, Faulkner LR (2001) *Electrochemical methods: fundamentals and applications*, 2nd edn. Wiley, New York
33. Brown AP, Anson FC (1977) *Anal Chem* 49:1589
34. Schlereth DD, Schuhmann W, Schmidt HL (1995) *J Electroanal Chem* 381:63
35. Puskas Z, Inzelt G (2005) *Electrochim Acta* 50:1481
36. Meites L (1965) *Polarographic techniques*, 2nd edn. Wiley, New York, pp 282–284
37. Bond AM (1980) *Modern polarographic methods in analytical chemistry*. Marcel Dekker, New York, pp 29–30
38. Kobayashi N, Matsue T, Fujihira M, Osa T (1979) *J Electroanal Chem* 103:427
39. Kobayashi N, Nishiyama Y (1984) *J Electroanal Chem* 181:107
40. Bettelheim A, Chan R JH, Kuwana T (1980) *J Electroanal Chem* 110:93
41. Li YP, Cao HB, Zhang Y (2006) *Chemosphere* 63:359
42. Lexa D, Saveant JM, Wang DL (1986) *Organometallics* 5:1428
43. Zheng GD, Yan Y, Gao S, Tong SL, Gao D, Zhen K Jr (1996) *Electrochim Acta* 41:177
44. Vilchez Aguado F, Gutierrez Granados S, Sucar Succar S, Bied-Charreton C, Bedioui F (1997) *New J Chem* 21:1009
45. Zheng G, Stradiotto M, Li L (1998) *J Electroanal Chem* 453:79
46. Ordaz AA, Bedioui F (1999) *Sens Actuators B* 59:128